Soil Dynamics and Earthquake Engineering 165 (2023) 107706

Contents lists available at ScienceDirect

Soil Dynamics and Earthquake Engineering

journal homepage: www.elsevier.com/locate/soildyn

Probabilistic prediction of ground-motion intensity for regions lacking strong ground-motion records

Yan-Gang Zhao [a,b], Rui Zhang [a], Haizhong Zhang [b,*]

[a] Key Laboratory of Urban Security and Disaster Engineering of Ministry of Education, Beijing University of Technology, Beijing, 100124, China
[b] Department of Architecture, Kanagawa University, 3-27-1 Rokkakubashi, Kanagawa-ku, Yokohama, 211-8686, Japan

ARTICLE INFO

Editor name - Dong-Sheng Jeng

Keywords:
Probabilistic prediction
Ground-motion intensity
Probabilistic seismic hazard analysis
Fourier amplitude spectrum
Random vibration theory
Monte Carlo simulation

ABSTRACT

Probabilistic prediction of ground-motion intensity in regions lacking strong ground-motion records is a vital issue for seismic structural design. Several approaches have been suggested for this purpose, and nearly all of them directly import and adjust the ground-motion prediction equation (GMPE) of ground-motion measures such as the peak ground acceleration (PGA) or spectral acceleration (*SA*) from data-rich regions. However, as the transmissions of PGA and *SA* from the source to the site correspond to nonlinear processes, this import and adjustment may lead to an unrealistic evaluation of ground motion. In this study, a novel probabilistic prediction method of ground-motion intensity for such regions is proposed. In contrast to the current approach wherein the GMPE of ground-motion measures such as PGA or *SA* is directly used, a Fourier amplitude spectral (FAS) model is suggested to express the seismic transmission process from the source to the site. The ground-motion intensities of PGA or *SA* are obtained from the FAS model using the random vibration theory. The exceedance probability of ground-motion intensity is calculated based on Monte Carlo simulations. As the FAS conforms to the linear system theory and the determination of FAS model does not require too many ground-motion records, the proposed method should be convenient for the probabilistic prediction of ground-motion intensity in regions lacking strong ground-motion records.

1. Introduction

Probabilistic seismic hazard analysis (PSHA) is a basic tool used to determine seismic action in structural design [1–3]. Probabilistic prediction of ground-motion intensity is the core of PSHA. When conducting a probabilistic prediction of ground-motion intensity, a ground-motion prediction equation (GMPE) is typically required for ground-motion intensity estimation at a site of interest using measures such as peak ground acceleration (PGA) or spectral acceleration (*SA*) [4–8]. The GMPEs are typically derived based on regression analysis of earthquake data, considering several predictive variables (such as magnitude, and source-to-site distance, etc.) and a functional form [9–19]. This process is usually available for seismically active regions with earthquake data [16]. However, it is difficult to develop reliable empirical GMPE in regions that lack strong ground-motion records worldwide [20]. To perform seismic hazard studies in these regions, usual practice involves the use of GMPEs from other regions. The selection of a particular GMPE for a specific region is not straightforward and is often based on a subjective decision of the hazard analyst. Not accounting for changes in regional seismological attributes, such as source, path, and site condition, can often lead to an unrealistic estimate of ground motion [21].

To solve this problem, several approaches have been suggested, such as direct "import" and "host-to-target" adjustments of GMPE for PGA or *SA* from data-rich regions [14,22–25]. However, the scaling of PGA or *SA* from the source to the site is inconsistent with the linear system theory, such that the import and adjustment do not purely reflect the differences between the host (data-rich) and target (data-poor) regions [26]. Therefore, probabilistic prediction of ground-motion intensity for regions lacking strong ground-motion records remains a challenge [21,27–30].

In this study, a new probabilistic prediction method of ground-motion intensity is proposed for regions lacking strong ground-motion records. In contrast to the current approach wherein the GMPE of ground-motion measures, such as PGA or *SA*, are directly used, a Fourier amplitude spectral (FAS) model is proposed to express the seismic transmission process from the source to the site, and ground-motion intensity, such as PGA or *SA*, is obtained from FAS using random

* Corresponding author.
E-mail address: zhang@kanagawa-u.ac.jp (H. Zhang).

https://doi.org/10.1016/j.soildyn.2022.107706
Received 14 August 2022; Received in revised form 6 December 2022; Accepted 6 December 2022

vibration theory (RVT). The remainder of this paper is organized as follows. Section 2 briefly reviews the current probabilistic prediction method of ground-motion intensity. In Section 3, the basic idea is described, an FAS model is introduced, calculations of PGA and *SA* from FAS are performed, and the procedure for calculating the exceedance probability of ground motion is summarized. Section 4 presents two examples to demonstrate the validity of the proposed method. Finally, the conclusions of this study are summarized in Section 5.

2. Review on probabilistic prediction of ground-motion intensity

After the potential seismic sources that may affect the site of interest are identified, the probability of ground-motion intensity exceeding a specific level over time t [2], $P(IM > im; t)$, can be obtained by

$$P(IM > im;\ t) = 1 - \prod_{k=1}^{\infty}[1 - P_k(IM > im;\ t)] \tag{1}$$

where IM is the ground-motion intensity measure, such as PGA or *SA*, im is a specific level ground-motion intensity measure, t is the time interval (year), k refers to the kth earthquake, and $P_k(IM > im; t)$ is the probability that the ground-motion intensity IM exceeds a specific level im over time t in the kth earthquake.

Assuming the Poisson model, $P_k(IM > im; t)$ is given by [31].

$$P_k(IM > im;\ t) = 1 - e^{-p_k v_k t} \tag{2}$$

where v_k is the mean annual rate of the kth earthquake, and p_k is the conditional probability that the seismic intensity IM exceeds level im given the occurrence of the kth earthquake. Considering m and r as random variables, p_k is expressed as [32].

$$p_k = \int_M \int_R P_{k\cdot im}(IM > im|m, r) f_M(m) f_R(r) dm dr \tag{3}$$

where $f_R(r)$ is the probability density function (PDF) of the source-to-site distance, and $f_M(m)$ is the PDF of the magnitude.

Typically, the truncated exponential recurrence model for $f_M(m)$ is used, which is expressed as [31].

$$f_M(m) = \frac{\theta e^{-\theta m}}{\theta e^{-\theta m_{min}} - \theta e^{-\theta m_{max}}} \tag{4}$$

where $m_{\min}$ is the minimum threshold magnitude, $m_{\max}$ is the maximum threshold magnitude, θ is statistical parameter, and $\theta = b\ln 10$, where b is the Gutenberg–Richter's parameter [33].

The PDF of R, $f_R(r)$ depends on the considered sources. For line and planar sources, the probability of earthquake occurrence is assumed to be uniformly distributed in the sources [34].

From the process outlined above, it is clear that the calculation of IM in Eq. (3) is a key step in the probabilistic prediction of ground-motion intensity. To obtain $P_{k\cdot im}(IM > im|m, r)$, one needs to know the mathematical model of the ground-motion intensity IM, referred to as the GMPE, expressed as a function of several seismological parameters of an earthquake, such as the magnitude and source-to-site distance. The GMPEs for PGA and *SA* are typically derived based on regression analysis of numerous earthquake data and on considerations of several predictive variables (such as magnitude and source-to-site distance, etc.) and a functional form [18]. The basic functional form of GMPE is expressed as follows:

$$\ln(\text{PGA or } SA) = \ln\left[\text{PGA or } SA(m, r, \text{other seismological parameters})\right]_p + \ln\varepsilon \tag{5}$$

where $\ln[\text{PGA or } SA\ (m, r, \text{other seismological parameters})]_p$ is the mean value of ln(PGA or *SA*), $\ln\varepsilon$ describes the difference between the actual ln (PGA or *SA*) and the predicted $\ln[\text{PGA or } SA\ (m, r, \text{other seismological parameters})]_p$. Many GMPEs have been developed [9,13,14,18], and can be found in Douglas [35].

Given that the abovementioned GMPEs are obtained from strong ground-motion records, the process is only available to seismically active regions with a mass of earthquake data, such as the Western United States [16], Taiwan [36], and Japan [37]. However, it is difficult to develop reliable empirical GMPEs in regions lacking strong ground-motion records worldwide (e.g., India) [20] using the same process. To probabilistically predict the ground-motion intensity in regions that have a paucity of strong ground-motion records, several approaches have been suggested.

One approach is "host-to-target" adjustment. Campbell [23] proposed a hybrid empirical method to adjust an empirically derived GMPE in data-rich (host) to data-poor (target) regions using the ratios of stochastically simulated response spectral ordinates in the target and host regions. Atkinson [14] also utilized response spectral ratios to adjust the GMPE, however, its form in the target and host regions was determined from the observed data. However, the scaling of response spectra from source to site is inconsistent with the linear system theory, and the response spectral ratios do not purely reflect the differences between the host and target regions. Therefore, the identification of specific extent adjustment factors (based on response spectral ratios) that can fully accommodate the true differences in seismological parameters in target and host regions remains an issue of debate [26].

Another approach involves the selection of GMPEs from data-rich (host) regions and the identification of a new GMPE based on the weighted average of the selected GMPEs [22,24,25]. However, the selection of many GMPEs for a site of interest is not straightforward, and often depends on the subjective decision of the hazard analyst. In addition, this approach does not account for changes in regional seismological attributes such as source, path, and site conditions, and can lead to an unrealistic estimate of ground-motion intensity [21].

Therefore, the probabilistic prediction of ground-motion intensity in regions lacking strong ground-motion records remains a challenging problem. Correspondingly, the objective of this study is to propose an effective method for the probabilistic prediction of ground-motion intensity for these regions.

3. Proposed probabilistic prediction method of ground motion intensity

3.1. Basic idea

From the discussion presented above, to obtain the exceedance probability of ground-motion intensity measures, such as PGA or *SA*, in regions lacking strong ground-motion records, almost all current methods directly import or adjust the GMPE of these measures (e.g., PGA or *SA*) in data-rich regions [14,22–25]. However, it has been pointed out that, for a dynamic system excited by a seismic motion, the ratio of the *SA* of the output motion to that of the incident motion, i.e., the transfer function of *SA*, is not purely determined by the system itself; however, it varies with the input motion, even for linear materials [26,38–40]. This indicates that the scaling of *SA* from source to ground is a nonlinear process and is inconsistent with the linear system theory. Therefore, direct importing of the GMPEs of PGA or *SA* and adjusting them using a simple response spectral ratio is theoretically unreasonable and may lead to unrealistic evaluation of ground motion [21]. To overcome this limitation, instead of directly using the ground-motion intensity measure (such as PGA or *SA*), one needs to identify another quantity to characterize ground motion by avoiding the abovementioned limitation and easily transforming it into ground-motion intensity. It is well know that, for a dynamic system excited by a seismic motion, the ratio of the FAS of the output motion to that of the incident motion, i.e., the transfer function of FAS, is purely determined by the system itself and independent of the input motion for linear materials. This means that the scaling of FAS from the source to the site

conforms to linear system theory. In addition, the ground-motion intensity (such as PGA or *SA*) can be obtained from FAS based on RVT with ease [38–41]. Therefore, FAS should be a suitable quantity to characterize ground motion to satisfy the aforedescribed set requirements [41]. Many GMPEs of FAS have been developed based on regression using numerous earthquake records [21,30]. Nevertheless, to predict the probability of ground-motion intensity in regions lacking ground-motion records, instead of using GMPE of FAS, we will directly use an FAS model, which only requires a few ground-motion records to determine its parameters [42,43]. After the FAS model is obtained, ground-motion intensity (such as PGA or *SA*) can be expressed as a function of FAS based on RVT. The exceedance probability of ground-motion intensity is then calculated using Monte Carlo simulation (MCS). As the FAS model conforms to the linear system theory, the determination of the FAS model does not require many ground-motion records, and the proposed method should be convenient for the probabilistic prediction of ground-motion intensity in regions lacking strong ground-motion records.

3.2. FAS model

Many approaches can be used to obtain the FAS, and one of the simplest is to compute it from a point source in terms of the various sources, paths, and site parameters using seismology theory. This study utilizes this model by using the point source spectrum described by Boore [41]. This ground-motion model has been validated by comparison with observations from actual seismic records [41,44]. The FAS of ground-motion acceleration at the surface $Y(f)$, is expressed as an explicit function of the source term $E(M_0, f)$, propagation path term $P(R, f)$, and the site term $G(f)$, such that

$$Y(f) = E(M_0,f)P(R,f)G(f) \tag{6}$$

where f is the frequency, R is the source-to-site distance, and M_0 is the seismic moment, which can be related to moment magnitude M by

$$M_0 = 10^{1.5M+16.05} \tag{7}$$

The source terms $E(M_0, f)$ are commonly expressed by the Brune ω-squared point source spectrum, although many other source spectral models are equally valid [41]. Substituting the ω-squared point source spectrum and the expressions for the path and site terms into Eq. (6) yields

$$Y(f) = \left[0.78\frac{\pi}{\rho\beta^3}M_0\frac{f^2}{1+(f/f_c)^2}\right]\left[Z(R)\times\exp\left(\frac{-\pi fR}{Q(f)\beta}\right)\right][\exp(-\pi kf)A(f)] \tag{8}$$

where ρ is the mass density of the crust, β is the shear-wave velocity of the crust, $Z(R)$ represents the geometric attenuation, $Q(f)$ represents the anelastic attenuation, k is the diminution parameter, $A(f)$ represents the crust amplification, and f_c is the corner frequency representing the frequency below which the FAS decays, and is defined as

$$f_c = 4.9\times10^6\beta\left(\frac{\Delta\sigma}{M_0}\right)^{1/3} \tag{9}$$

where $\Delta\sigma$ is the stress drop.

The parameters of the FAS model in Eq. (8) may differ for different regions, which can influence the FAS results. For example, the stress drop $\Delta\sigma$ and diminution parameter k can influence high-frequency signal strength of the FAS and its fall-off, respectively, the geometric attenuation $Z(R)$ affects the overall strength in the FAS, and crust amplification $A(f)$ and anelastic attenuation $Q(f)$ influence the strength and overall shape in FAS [41]. Thus, determining these parameters for a specific region is important for deriving reasonable results. In many regions of the world such as the eastern North America (ENA), the parameters of the FAS model have been determined based on ground motions recorded in these regions. For example, the source parameters in the ENA including the mass density ρ, shear-wave velocity of the crust β [45,46], and stress drop $\Delta\sigma$ [13,26,42,47–49] have been systematically studied. In addition, the parameters related to the path in the ENA including the geometric attenuation $Z(R)$ and anelastic attenuation $Q(f)$ have been explored [41,45,50–52]. Moreover, the site parameters in the ENA including the diminution parameter k and crust amplification $A(f)$ have also been discussed [45,51,53,54]. For such regions with these parameters being fully discussed, the parameters of the FAS model can be obtained by directly refereeing to these studies. For regions whose parameters are not fully discussed, the parameters of the FAS model are to be determined based on ground motions recorded in these regions, following the inversion procedure of previous studies [42,43]. Because FAS conforms to linear system theory, the parameters of the FAS model can be reasonably determined based on limited earthquake data in regions lacking strong ground-motion records [23].

3.3. Calculation of PGA and SA from FAS

After the FAS model is obtained, one requires an effective procedure to obtain the PGA and *SA* from FAS. Herein, the RVT was applied. Based on this theory, the peak value of ground motion, response spectrum, and site response were evaluated [55]. The RVT describes the relationship between root-mean-square (RMS) and FAS. Using the FAS of ground motion, the peak acceleration of the corresponding time-domain motion is expressed as follows.

$$\mathrm{PGA} = pf\sqrt{\frac{1}{D\pi}\int_0^\infty |Y(\omega)|^2 d\omega} \tag{10}$$

where pf is the peak factor, D is the duration, ω is the circular frequency, and $\omega = 2\pi f$. The square root term in Eq. (10) represents the RMS acceleration according to Parseval's theorem.

Several peak factor models have been developed for RVT analyses [56–58]. Although the Cartwright and Longuet–Higgins [56] model has been commonly applied in engineering seismology and site-response analyses, the Vanmarcke [58] model can provide better estimations of the peak factor [59]. The cumulative distribution function of the peak factor, pf, provided by Vanmarcke [58] is expressed as follows.

$$P(pf<r) = \left[1-\exp\left(-r^2/2\right)\right]\exp\left[-2f_z\exp\left(-r^2/2\right)D\frac{1-\exp\left(-\delta^{1.2}r\sqrt{\pi/2}\right)}{1-\exp\left(r^2/2\right)}\right] \tag{11}$$

where δ is the bandwidth factor of FAS, which is defined as a function of the spectral moments of FAS as follows.

$$\delta = \sqrt{1-\frac{(m_1)^2}{m_0\bullet m_2}} \tag{12}$$

where m_n (n = 0, 1, 2) denotes the nth order spectral moment of the square of FAS, which is defined by

$$m_n = \frac{1}{\pi}\int_0^\infty \omega^n |Y(\omega)|^2 d\omega \tag{13}$$

where f_z is the rate of zero crossing, and it is defined as follows.

$$f_z = \frac{1}{2\pi}\sqrt{\frac{m_2}{m_0}} \tag{14}$$

In RVT analysis, the expected value of pf is typically used. According to Eq. (11), the expected value of pf, $\overline{pf}$, is obtained by

$$\overline{pf} = \int_0^\infty rP'(pf < r)dr = rP(pf < r)|_0^\infty - \int_0^\infty P(pf < r)dr = r|_0^\infty - \int_0^\infty P(pf < r)dr = \int_0^\infty 1 - P(pf < r)dr \tag{15}$$

where $P'(pf < r)$ is the PDF of pf.

Similar to the PGA, SA can be expressed based on RVT as

$$SA(\omega) = pf_{SA}\sqrt{\frac{1}{D_{rms}\pi}\int_0^\infty |Y_{SA}(\omega)|^2 d\omega} \tag{16}$$

where pf_{SA} and D_{rms} are the peak factor and duration of the oscillator response of ground motion, respectively. $Y_{SA}(\omega)$ is the FAS of the oscillator acceleration response spectra, and is expressed as

$$Y_{SA}(\omega) = Y(\omega)H_{SA}(\omega) \tag{17}$$

where $H_{SA}(\omega)$ is the oscillator transfer function for the acceleration response spectra, which can be expressed as follows,

$$H_{SA}(\omega) = \frac{\sqrt{(2\xi\omega\overline{\omega})^2 + (\overline{\omega})^4}}{\sqrt{(2\xi\omega\overline{\omega})^2 + \left(\omega^2 - (\overline{\omega})^2\right)^2}} \tag{18}$$

where $\overline{\omega}$ is the oscillator circular frequency, and ξ is the oscillator damping ratio.

The duration D_{rms} can be estimated from D. Several studies developed equations for D_{rms} [60,61]. The most recent D_{rms} was developed by Boore and Thompson [62], and is expressed as

$$D_{rms} = D\left(c_1 + c_2\frac{1-\eta^{c_3}}{1+\eta^{c_3}}\right)\left[1 + \frac{c_4}{2\pi\xi}\left(\frac{\eta}{1+c_5\eta^{c_6}}\right)^{c_7}\right] \tag{19}$$

where

$$\eta = \frac{2\pi}{\overline{\omega}D} \tag{20}$$

where c_i, $i = 1,2,\ldots,7$ are coefficients. Additional details can be found in Boore and Thompson [62].

According to Atkinson and Silva [63], the duration of the ground motion is defined as

$$D = \frac{1}{f_c} + 0.05R \tag{21}$$

3.4. Calculation of exceedance probability of ground motion

To calculate the probability of ground-motion intensity exceeding a specific level at a site of interest based on considerations of all possible earthquakes, the conditional probability that the seismic intensity IM exceeds level im given the occurrence of the kth earthquake (expressed in Eq. (3)) should be obtained. Instead of directly using IM, such as PGA or SA in Eq. (3), an FAS model expressed in Eq. (10) was used, accordingly, p_k can then be obtained without the GMPE of PGA or SA; however, with the use of numerous strong ground-motion records.

Substituting Eq. (10) into Eq. (3), the p_k for PGA can be obtained as follows:

$$p_k = \int_M\int_R P_{k\bullet im}\left(pf\sqrt{\frac{1}{D\pi}\int_0^\infty |Y(\omega)|^2 d\omega} > im \middle| m, r\right) f_M(m) f_R(r) dmdr \tag{22}$$

Substituting Eq. (16) into Eq. (3), the p_k value for SA can be obtained as

$$p_k = \int_M\int_R P_{k\bullet im}\left(pf_{SA}\sqrt{\frac{1}{D_{rms}\pi}\int_0^\infty |Y_{SA}(\omega)|^2 d\omega} > im \middle| m, r\right) f_M(m) f_R(r) dmdr \tag{23}$$

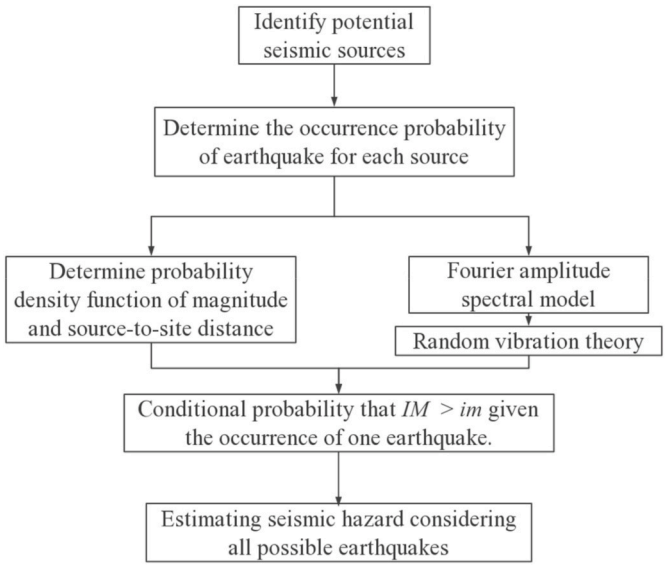

Fig. 1. Flowchart of the proposed probabilistic prediction method of ground motion.

Given that the integrands in Eqs. (22) and (23) are complicated, it is difficult to obtain theoretical solutions. Accordingly, MCS was used herein.

The basic steps of the proposed method are summarized as follows.

(1) Identify potential seismic sources that may affect the site of interest
(2) Determine the occurrence probability of earthquake for each source ν_k by using Eq. (2)
(3) Determine probabilistic models $f_M(m)$ and $f_R(r)$ by using Eq. (3)
(4) Determine the seismological parameters
(5) Use MCS to evaluate the probability that PGA and SA will exceed a certain level during a specified time for each earthquake
(6) Obtain the exceedance probability of ground motion at the site of interest considering contributions from all possible earthquakes.

The flowchart of the proposed method is shown in Fig. 1. Although the seismological parameters in the FAS model are required in the proposed approach, they can be determined using a small number of moderate earthquake records instead of strong earthquake records [42,43]. The determination of these seismological parameters can be found in previous studies [13,26,42,45–54].

It can be noted from Sections 3.1-3.4, in contrast to the traditional probabilistic prediction method of ground-motion intensity summarized in Section 2, where GMPE of ground-motion measures, such as PGA or SA, are directly used, the proposed procedure uses FAS to characterize the ground motion. Therefore, the transmission of PGA or SA from the source to ground, which does not conform to the linear system theory, is replaced by the transmission of FAS, which conforms to the linear system theory. Furthermore, the ground-motion intensity (such as PGA or SA) can be obtained from FAS based on RVT with ease. Therefore, the proposed procedure can simulate the nonlinear transmission process of PGA or SA while keeping a linear system characteristic of FAS. In addition, because FAS conforms to the linear system theory and determination of the FAS model does not require too many records, the proposed method should be convenient and effective for the probabilistic prediction of ground motion in regions lacking strong ground-motion records.

4. Numerical examples

In this section, two examples are used to demonstrate the validity of

Table 1
Probability information about the parameters used in the Fourier amplitude spectral model.

Parameters	Distribution	Mean	Standard deviation
Density of crust ρ (g/cm^3)	Lognormal	2.8	0.56
Stress drop $\Delta\sigma$ (bar)	Lognormal	400	100
Shear-wave velocity of crust β (km/s)	Lognormal	3.7	0.74
Site diminution k (s)	Lognormal	0.04	0.012

Table 2
Parameters used in the Fourier amplitude spectral model.

Parameters	value
Crust amplification $A(f)$	(Boore and Thompson 2015)
Geometrical spreading $Z(R)$	(Atkinson and Boore 2014)
Path attenuation	(Atkinson and Boore 2014)

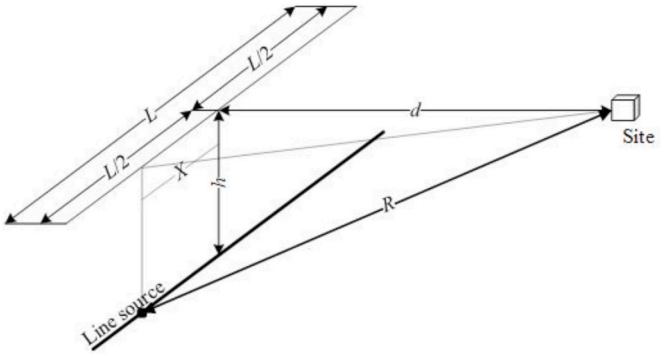

Fig. 2. Distribution of the considered site and seismic source.

the proposed method. Here, values of the parameters of the FAS model for the ENA regions were adopted [64] as listed in Tables 1 and 2. Because the parameters of the FAS model may vary for each region, these should be determined according to the specific region based on the procedure described in Section 3.2. The probabilistic information concerning the distribution of the parameters used in the FAS model are listed in Table 1.

Example 1. A line source

Example 1 considers a line source, as shown in Fig. 2. The length of the source L is 100 km, the depth of hypocenter h is 20 km, and the epicentral distance d is 10 km. In addition, the average occurrence rate ν of the line source is assumed to be equal to 0.02 per year with $M \geq 4$. The truncated exponential recurrence model is used as the PDF of magnitude, where the minimum threshold magnitude $m_{\min}$ is four, the maximum threshold magnitude $m_{\max}$ is eight, and the statistical parameter θ is 2.6. It is assumed that an earthquake occurs along with

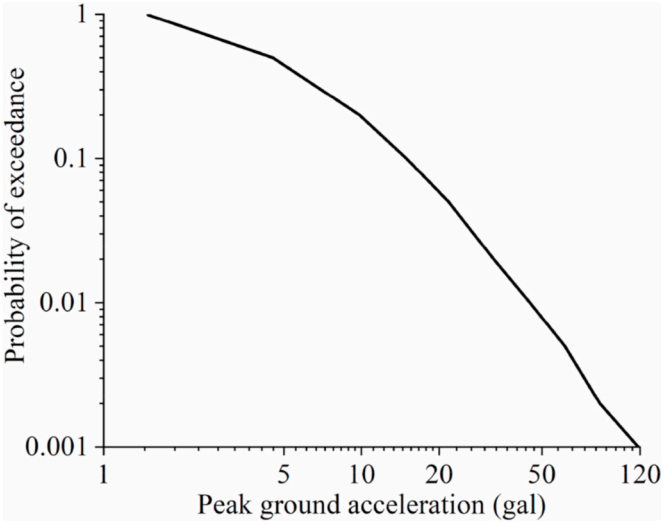

Fig. 3. Seismic hazard curve for peak ground acceleration obtained using Monte Carlo simulation (MSC) with 10000 samples.

the line source with a uniform distribution. The time interval t was considered equal to 50 years. In addition, 10 oscillator periods were considered ($T = 0.01$, 0.02, 0.05, 0.1, 0.2, 0.5, 1, 2, 5, and 10 s), and the oscillator damping ratio ξ was set to 0.05. In total, 10000 samplings were used in the MCS.

The basic process of obtaining the probability that ground-motion intensity IM exceeds a specific level im over time t, $P(IM > im; t)$, can be summarized as follows.

(1) Determine the PDFs of M and R, respectively.

The PDF of M is expressed as

$$f_M(m) = \frac{2.6e^{-2.6m}}{e^{-10.4} - e^{-20.8}} \tag{24}$$

and the PDF of R is expressed as

$$f_R(r) = \frac{2r}{L\sqrt{r^2 - (d^2 + h^2)}} \tag{25}$$

where $d^2 + h^2 \leq r \leq d^2 + h^2 + (L/2)^2$.

(2) Calculate the PGA and SA from the FAS model based on the method presented in Section 3.4
(3) Calculate the conditional probability p_k expressed in Eqs. (22) and (23) using MSC
(4) Calculate the exceedance probability P_k expressed by Eq. (2)

Table 3
Probabilities of exceedance for peak ground acceleration (PGA) and spectral acceleration (SA).

Exceedance Probability	PGA (gal)	SA (gal)									
		0.01 s	0.02 s	0.05 s	0.1 s	0.2 s	0.5 s	1 s	2 s	5 s	10 s
0.99	1.5	0.6	0.6	0.9	1.6	1.1	0.3	0.05	0.01	0.001	0.0003
0.5	4.5	1.8	1.8	3.3	5.0	2.1	0.6	0.1	0.02	0.003	0.0007
0.2	9.8	4.1	4.2	7.8	11.0	4.2	1.5	0.4	0.07	0.008	0.002
0.1	14.9	6.4	6.6	11.9	17.1	6.6	2.8	0.8	0.2	0.02	0.004
0.05	21.8	9.6	9.9	17.4	24.8	9.5	4.8	1.6	0.4	0.04	0.009
0.02	32.6	15.1	15.5	26.6	36.8	15.4	9.2	3.8	1.0	0.1	0.02
0.01	44.9	22	22.6	37.7	53.4	21.5	13.6	6.3	1.9	0.2	0.05
0.005	61.4	30.8	31.5	52.7	72.4	30.3	20.4	10.5	3.8	0.5	0.10
0.002	83.9	48	48.6	79.0	105.8	43.9	31.4	17.8	7.5	1.3	0.3
0.001	118.1	72.5	73.4	106.6	159.0	52.5	38.2	22.6	10.0	2.0	0.4

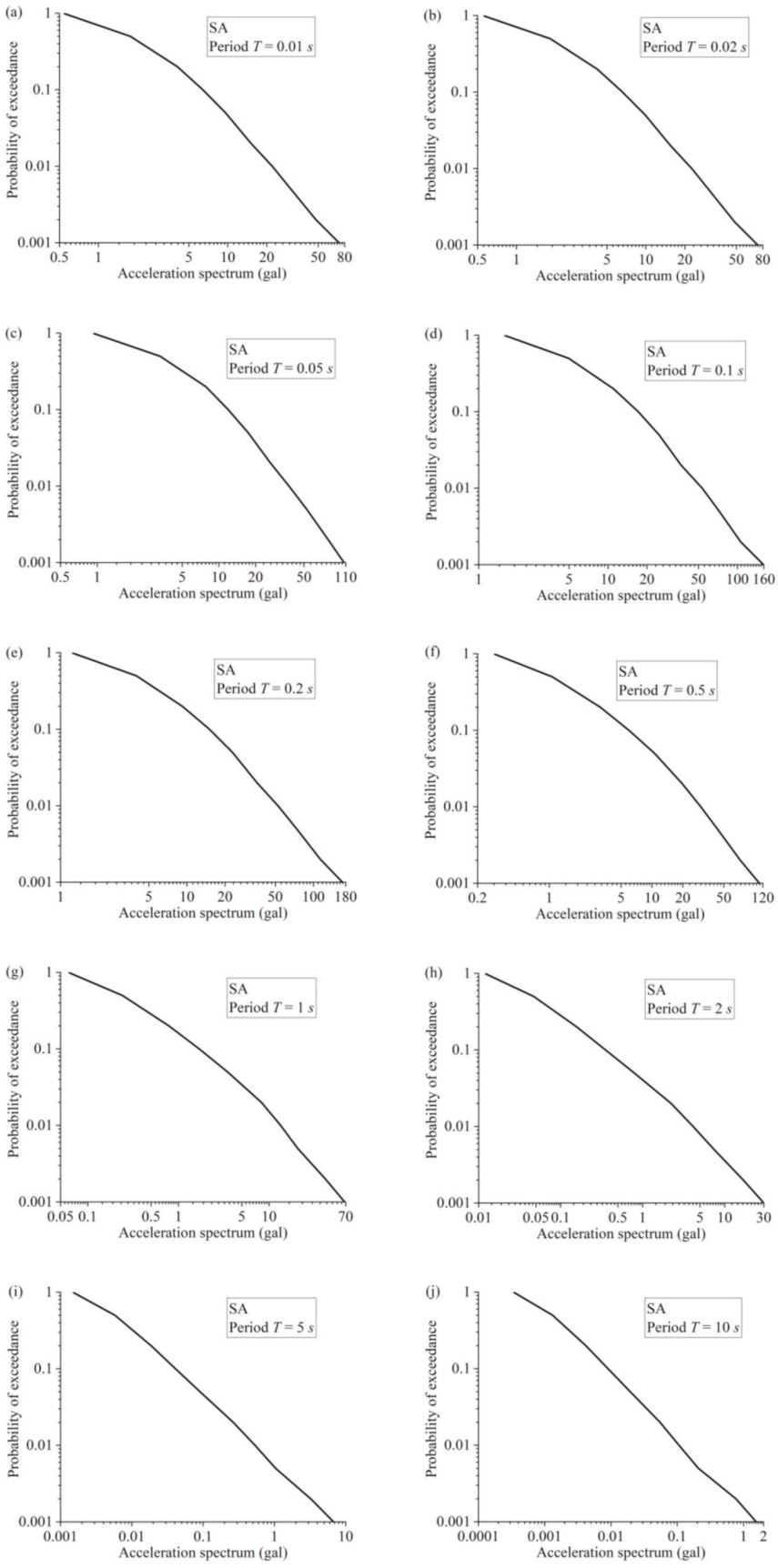

Fig. 4. Seismic hazard curve for spectral acceleration (*SA*) obtained using MCS with 10000 samples.

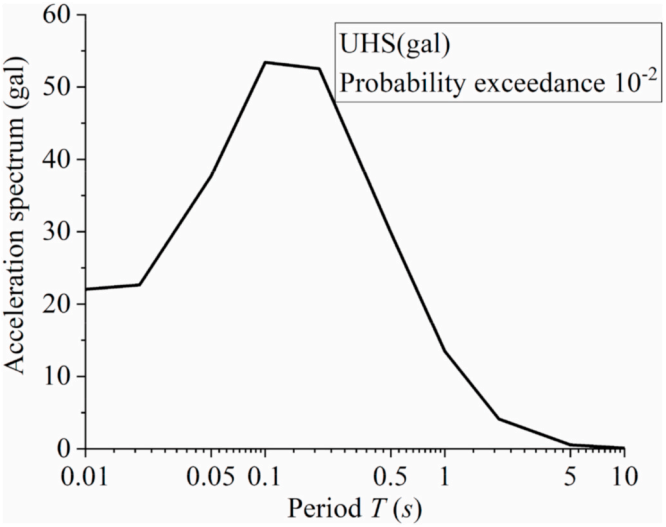

Fig. 5. Uniform hazard spectrum (UHS) obtained using MCS with 10000 samples.

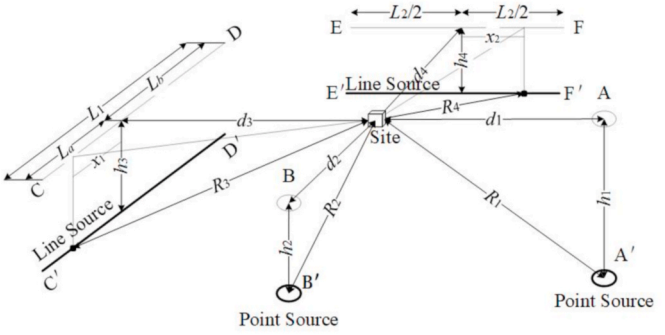

Fig. 6. Distribution of the site and seismic sources.

The calculation results of exceedance probability for PGA and *SA* are listed in Table 3. The hazard curve of PGA is shown in Fig. 3, and the hazard curves of *SA* are shown in Fig. 4.

After obtaining the exceedance probability of *SA* in specific frequencies, the value of uniform hazard spectrum (UHS) of the specific exceedance probability can be obtained. In this example, the UHS for exceedance probability of 10^{-2} was estimated, as shown in Fig. 5.

Example 2. Multiple seismic sources

The second example considers four sources, including two point sources and two line sources, as shown in Fig. 6. The A' and B' represent two point sources, and $C'D'$, $E'F'$ represent two line sources. For the point source A', the hypocenter depth h_1 is 20 km, and the epicentral distance d_1 is 30 km. For the point source B', the hypocenter depth h_2 is 15 km, and the epicentral distance d_2 is 50 km. For the line source $C'D'$, the length of fault $L_1 = L_a + L_b$ is 100 km, where L_a is 30 km, L_b is 70 km, the hypocenter depth h_3 is 20 km, and the minimum distance between the surface projection of the fault and site d_3 is 35 km. For the line source $E'F'$, the length of fault L_2 is 120 km, the hypocenter depth h_4 is 25 km, and the minimum distance between the surface projection of the fault and the site d_4 is 50 km. The average occurrence rate of ν_1 is 0.04 for source A', ν_2 is 0.06 for source B', ν_3 is 0.12 for source $C'D'$, and ν_4 is 0.08 for source $E'F'$ per year with $M \geq 6$. The statistical parameter θ is 2.6 and the time interval t is 50 years. The density of crust ρ is 2.8 g/cm^3, stress drop $\Delta\sigma$ is 400 bar, shear-wave velocity of crust β is 3.7 km/s, and site diminution k is 0.04 s. The other parameters of FAS model are listed in Table 2. It was assumed that an earthquake occurs along the line source with a uniform distribution. In addition, 10 oscillator periods were also considered (i.e., $T = 0.01$, 0.02, 0.05, 0.1, 0.2, 0.5, 1, 2, 5, 10 s), and the oscillator damping ratio ξ was set to 0.05.

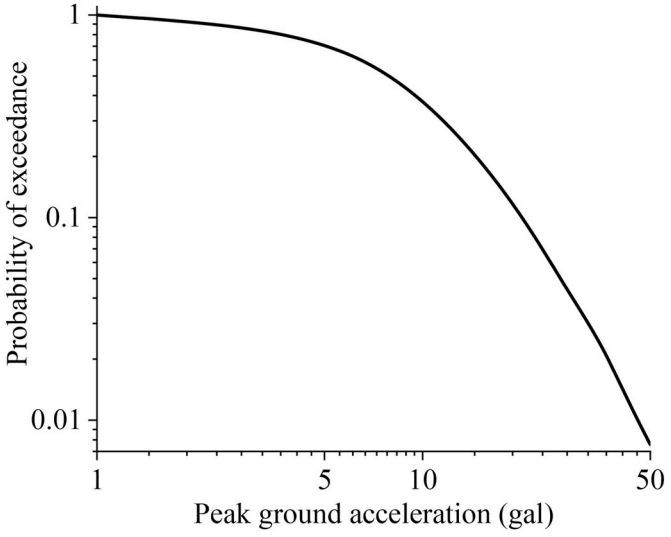

Fig. 7. Seismic hazard curve for peak ground acceleration obtained using MCS with 10000 samples.

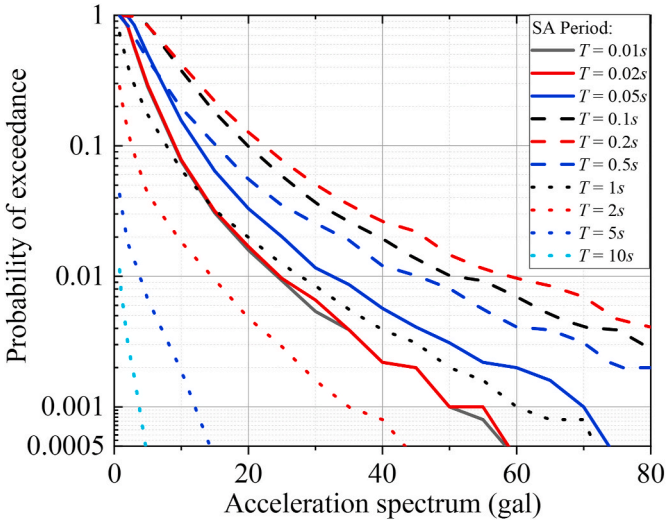

Fig. 8. Seismic hazard curve for spectral acceleration (*SA*) obtained using MCS with 10000 samples.

Using MCS with 10000 samples, the probabilities of exceedance for the PGA and *SA* are shown in Figs. 7 and 8, respectively. Fig. 8 shows that when the exceedance probability of the *SA* is less than 0.001 (usually 10% of the number of MCS samplings), the hazard curves become zigzagged. This is because the number of samplings in MCS is only 10000, and the results are unstable when the exceedance probability is significantly small. Increasing the number of samplings of MCS can avoid this problem.

When the probability of exceedance for *SA* is obtained, the UHS of a specific exceedance probability can be estimated. In this example, the UHS for exceedance probabilities of 10^{-1}, 10^{-2}, and 10^{-3} were estimated, as shown in Fig. 9.

From the two examples, the proposed method is a useful probabilistic prediction tool of ground-motion intensity for regions lacking strong ground-motion records. Since multiple integrals are required in Eq. (22) or (23), and Monte Carlo Simulation is used to calculate the exceedance probability, the computational efficacy needs to be improved when a small exceedance probability is of interest.

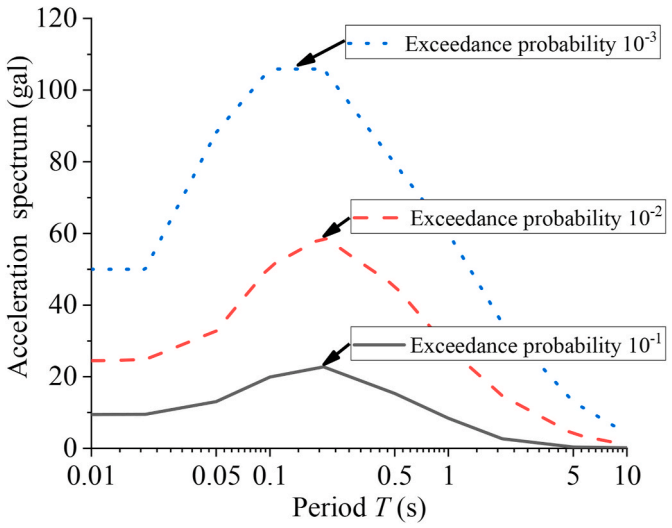

Fig. 9. Uniform hazard spectrum (UHS) obtained using MCS with 10000 samples.

5. Conclusion

In this study, a probabilistic prediction method of ground-motion intensity for regions lacking strong ground-motion records was proposed. This method is in contrast different from the current probabilistic prediction method of ground-motion intensity summarized in Section 2, where the GMPE of ground-motion measures such as the PGA or *SA* are directly used. An FAS model is suggested to express the seismic transmission process from the source to the site. The PGA and *SA* were then obtained from FAS based on the RVT. Because the FAS model conforms to the linear system theory and the determination of the FAS model does not require many records, the proposed method is feasible in regions lacking strong ground-motion records. The numerical examples show that the method is convenient and effective as a probabilistic prediction tool of ground-motion intensity for regions lacking strong ground motion records.

Funding

This study was partially funded by the National Natural Science Foundation of China (Grant Number 51738001and 5227813).

Conflicts of interest/Competing interests

The authors have no conflicts of interest to declare that are relevant to the content of this article.

Author statement

Yan-Gang Zhao: Conceptualization, Methodology, Writing- Reviewing and Editing.

Rui Zhang: Conceptualization, Methodology, Writing-Original draft preparation, Data curation, Visualization.

Haizhong Zhang: Conceptualization, Methodology, Writing-Reviewing and Editing.

Code availability

Available upon request.

Authors' contributions

Yan-Gang Zhao: data curation, supervision, writing-reviewing and editing. Rui Zhang: data curation, writing-original draft preparation, visualization, conceptualization, methodology. Haizhong Zhang: writing-reviewing and editing, conceptualization, methodology, investigation, supervision.

Declaration of competing interest

The authors declare that they have no known competing financial interests or personal relationships that could have appeared to influence the work reported in this paper.

Data availability

Data will be made available on request.

Acknowledgments

We acknowledge the support received from the National Natural Science Foundation of China in ensuring the success of this study.

References

[1] Eurocode 8. Design of structures for earthquake resistance, part 1: general rules, seismic actions and rules for buildings, EN 2004-1-1. Brussels, Belgium: European Committee for Standardization (CEN); 2004.
[2] Fujiwara H, Kawai S, Aoi S, Morikawa N, Senna S, Kobayashi K, Ishii T, Okumura T, Hayakawa Y. National seismic hazard maps for Japan. 81. Bulletin of Earthquake Research Institute, University of Tokyo; 2006. p. 221–32.
[3] GB 18306. Seismic ground motion parameters zonation map of China. Beijing: China Building Industry Press; 2015 (In Chinese); 2015.
[4] Farman MS, Said A. Updated probabilistic seismic hazard assessment for Iraq. Civ. Eng. J. 2018;4(7):1610.
[5] Das R, Gonzalez G, Llera J, Saez E, Meneses C. A probabilistic seismic hazard assessment of southern Peru and Northern Chile. Eng Geol 2020;271:105585.
[6] Keshri CK, Mohanty WK, Ranjan P. Probabilistic seismic hazard assessment for some parts of the Indo-Gangetic plains, India. Nat Hazards 2020;103(2):815–43.
[7] Li B, Srensen MB, Atakan K, Li Y, Li Z. Probabilistic seismic hazard assessment for the Shanxi Rift system, North China. Bull Seismol Soc Am 2020;110(1):127–53.
[8] Yousuf M, Bukhari K. Hazard estimation of Kashmir Basin, NW Himalaya using probabilistic seismic hazard assessment. Acta Geophys. 2020;69(4):1–22.
[9] Esteva L, Rosenblueth E. Espectros de temblores a distancias moderadas y grandes. Sociedad Mexicana de Ingenieria Sismica 1964;1(2):1–18.
[10] Esteva L. Seismic risk and seismic design decisions. In: Hansen RJ, editor. Seismic design for nuclear power plants. USA: MIT Press; 1970.
[11] Campbell KW. Empirical near-source attenuation relationships for horizontal and vertical components of peak ground acceleration, peak ground velocity, and pseudo-absolute acceleration response spectra. Seismol Res Lett 1997;68(1):154–79.
[12] Midorikawa S, Fujimoto K, Muramatsu I. Correlation of new J.M.A. instrumental seismic intensity with former J.M.A. seismic intensity and ground motion parameters. J Soc Saf Sci 1999:51–6.
[13] Atkinson GM, Boore DM. Earthquake ground-motion prediction equations for eastern north America. Bull Seismol Soc Am 2006;96(6):2181–205.
[14] Atkinson GM. Ground-Motion prediction equations for eastern north America from a referenced empirical approach: implications for epistemic uncertainty. Bull Seismol Soc Am 2008;98(3):1304–18.
[15] Boore DM, Atkinson GM. Ground-motion prediction equations for the average horizontal component of PGA, PGV, and 5%-damped PSA at spectral periods between 0.01 *s* and 10.0 *s*. Earthq Spectra 2008;24(1):99–138.
[16] Campbell KW, Bozorgnia Y. NGA-West2 ground motion model for the average horizontal components of PGA, PGV, and 5% damped linear acceleration response spectra. Earthq Spectra 2014;30(3):1087–115.
[17] Vladimir Graizer. Ground-motion prediction equations for central and eastern north America. Bull Seismol Soc Am 2016;106(4):1600–12.
[18] Mori T, Shigefuji M, Bijukchhen S, Kanno T, Takai N. Ground motion prediction equation for the Kathmandu Valley, Nepal based on strong motion records during the 2015 Gorkha Nepal earthquake sequence. Soil Dynam Earthq Eng 2020;135:106208.
[19] Ge FW, Tong MN, Zhao YG. A structural demand model for seismic fragility analysis based on three-parameter lognormal distribution. Soil Dynam Earthq Eng 2021;147(6):106770.
[20] Kanth S, Iyengar RN. Estimation of seismic spectral acceleration in Peninsular India. J Earth Syst Sci 2007;116(3):199–214.
[21] Bora SS, Scherbaum F, Kuehn N, Stafford P. Fourier spectral- and duration models for the generation of response spectra adjustable to different source-, propagation-, and site conditions. Bull Earthq Eng 2014;12(1):467–93.
[22] Kulkarni RB, Youngs RR, Coppersmith KJ. Assessment of confidence intervals for results of seismic hazard analysis. Proceedings of Eighth World Conference on Earthquake Engineering. San Francisco 1984;(1):263–70.

[23] Campbell KW. Prediction of strong ground motion using the hybrid empirical method and its use in the development of ground-motion (attenuation) relations in Eastern North America. Bull Seismol Soc Am 2003;93(3):1012–33.
[24] Cotton F, Scherbaum F, Bommer JJ, Bungum H. Criteria for selecting and adjusting ground-motion models for specific target regions: application to central Europe and rock sites. J Seismol 2006;10(2):137.
[25] Bommer JJ, Douglas J, Scherbaum F, Cotton F, Bungum H, Fah D. On the selection of ground-motion prediction equations for seismic hazard analysis. Seismol Res Lett 2010;81(5):783–93.
[26] Bora SS, Scherbaum F, Kuehn N, Stafford P. On the relationship between Fourier and response spectra: implications for the adjustment of empirical ground-motion prediction equations (GMPEs). Bull Seismol Soc Am 2016;106(3):1235–53.
[27] Eftekhari N, Sayyadpour H, Kowsari M. A near-fault probabilistic seismic hazard assessment for Yasouj, located in the Kazerun fault system, southwest Iran. Nat Hazards 2020;105:1945–61.
[28] Poggi V, Garcia-Peláez Julio, Styron R, Pagani M, Gee R. A probabilistic seismic hazard model for North Africa. Bull Earthq Eng 2020;18(1):2917–51.
[29] Rahman AU, Rasheed A, Najam FA, Zaman S, Khan SU. An updated earthquake catalogue and source model for seismic hazard analysis of Pakistan. Arabian J Sci Eng 2021;46:5219–41.
[30] Vemula S, Raghukanth STG, Ponnalagu A. Fourier amplitude spectrum prediction and generation of synthetic ground motion to New Zealand. Acta Geophys. 2022;(1).
[31] Cornell CA. Engineering seismic risk analysis. Bull Seismol Soc Am 1968;58(5):1583–606.
[32] McGuire RK. FORTRAN computer program for seismic risk analysis. U.S Geol Surv Open-File Rep 1976;76(67):90. VA; 1976;.
[33] Gupta ID. The state of the art in seismic hazard analysis. ISET J Earthq Technol 2002;39(4):311–46.
[34] Alamilla JL, Rodriguez JA, Vai R. Unification of different approaches to probabilistic seismic hazard analysis. Bull Seismol Soc Am 2020;110(6):2816–27.
[35] Douglas J. Ground motion prediction equations 1964-2021. http://www.gmpe.org.uk/; 2021.
[36] Phung VB, Loh CH, Shu HC, Abrahamson NA. Ground motion prediction equation for Taiwan subduction zone earthquakes. Earthq Spectra 2020;36(3):1331–58.
[37] Si H, Midorikawa S. New attenuation relations for peak ground acceleration and velocity considering effects of fault type and site condition. Auckland. In: Proceedings of the 12th world conference on earthquake engineering; 2000. paper No. 532.
[38] Stafford PJ, Rodriguez-Marek A, Edwards B, Kruiver PP, Bommer JJ. Scenario dependence of linear site-effect factors for short-period response spectral ordinates. Bull Seismol Soc Am 2017;107(6):2859–72.
[39] Zhang HZ, Zhao YG. Analytical model for response spectral ratio considering the effect of earthquake scenarios. Bull Earthq Eng 2021;19:5285–305.
[40] Zhang HZ, Zhao YG. Effects of earthquake magnitude, distance, and site conditions on spectral and pseudospectral velocity relationship. Bull Seismol Soc Am 2021;111(6):3160–74.
[41] Boore DM. Simulation of ground motion using the stochastic method. Pure Appl Geophys 2003;160(3–4):635–76.
[42] Boore DM. Ground motion models for very-hard-rock sites in Eastern North America: an update. Seismol Res Lett 2018;89(3):1172–84.
[43] Boore DM. Revision of Boore (2018) ground-motion predictions for Central and Eastern North America: path and offset adjustments and extension to 200 m/s≤VS30≤3000 m/s. Seismol Res Lett 2020;91(2A):977–91.
[44] Boore DM. Stochastic simulation of high-frequency ground motions based on seismological models of the radiated spectra. Bull Seismol Soc Am 1983;73(6):1865–94.
[45] Boore DM, Joyner WB. Site amplifications for generic rock sites. Bull Seismol Soc Am 1997;87:327–41.
[46] Somerville P, Collins N, Graves R, Saikia C. Ground motion attenuation relations for the central and Eastern United States. Report to U.S. Geological survey, NEHRP external research program, Award No. 99-HQ-GR-0098.
[47] Atkinson GM, Beresnev I. Don't call it stress drop. Seismol Res Lett 1997;68(1):3–4.
[48] Yenier E, Atkinson GM. Regionally adjustable generic ground-motion prediction equation based on equivalent point-source simulations: application to central and eastern North America. Bull Seismol Soc Am 2015;105(4):1989–2009.
[49] Boore DM. SMSIM—fortran programs for simulating ground motions from earthquakes: version 2.3-A revision of OFR 96-80-A, U.S. Geological Survey Open-File Report. 00-509, revised 15 August. 2005. p. 55.
[50] Atkinson M, Mereu RF. The shape of ground motion attenuation curves in southeastern Canada. Bull Seismol Soc Am 1992;82(5):2014–31.
[51] Atkinson GM. Empirical attenuation of ground-motion spectral amplitudes in Southeastern Canada and the Northeastern United States. Bull Seismol Soc Am 2004;94(3):1079–95.
[52] Atkinson GM, Boore DM. The attenuation of Fourier amplitudes for rock sites in eastern North America. Bull Seismol Soc Am 2014;104:513–28.
[53] Atkinson GM. The high-frequency shape of the source spectrum for earthquakes in eastern and western Canada. Bull Seismol Soc Am 1996;86:106–12.
[54] Siddiqqi J, Atkinson GM. Ground-motion amplification at rock sites across Canada as determined from the horizontal-to-vertical component ratio. Bull Seismol Soc Am 2002;92(2):877–84.
[55] Hanks TC, Mcguire RK. The character of high-frequency strong ground motion. Bull Seismol Soc Am 1981;71(3):1897–919.
[56] Cartwright DE, Longuet-Higgins MS. The statistical distribution of the maxima of a random function. Proc Royal Soc London. Ser A, Math Phys Sci 1956;237(1209):212–32.
[57] Davenport AG. Note on the distribution of the largest value of a random function with applications to rust loading. Proc Inst Civ Eng 1964;28(2):187–96.
[58] Vanmarcke EH. Distribution of first-passage time for normal stationary random processes. J Appl Mech 1975;42(1):215–20.
[59] Palermo M, Silvestri S, Trombetti T. Stochastic-based damping reduction factors. Soil Dynam Earthq Eng 2016;80:168–76.
[60] Boore DM, Joyner WB. A note on the use of random vibration theory to predict peak amplitudes of transient signals. Bull Seismol Soc Am 1984;74(5):2035–9.
[61] Liu L, Pezeshk S. An improvement on the estimation of pseudoresponse spectral velocity using RVT method. Bull Seismol Soc Am 1999;89(5):1384–9.
[62] Boore DM, Thompson EM. Revisions to some parameters used in stochastic-method simulations of ground motion. Bull Seismol Soc Am 2015;105(2A):1029–41.
[63] Atkinson GM, Silva W. Stochastic modeling of California ground motions. Bull Seismol Soc Am 2000;90(2):255–74.
[64] Zhang HZ, Zhao YG. Damping modification factor based on random vibration theory using a source-based ground-motion model. Soil Dynam Earthq Eng 2020;136:106225.